Available online at www.sciencedirect.com
ScienceDirect
Energy Procedia 73 (2015) 263 – 271
Energy Procedia

9th International Renewable Energy Storage Conference, IRES 2015

Thermochemical heat storage at high temperatures using Mn_2O_3/Mn_3O_4 system: narrowing the redox hysteresis by metal co-doping

Alfonso J. Carrillo,[a] David P. Serrano,[a, b] Patricia Pizarro[a, b] and Juan M. Coronado[a]*

[a]*Thermochemical Processes Unit, IMDEA Energy Institute, Avenida Ramón de la Sagra, 3, Parque Tecnológico de Móstoles, 28935. Móstoles, Madrid, Spain.*
[b]*Chemical and Environmental Engineering Group, ESCET, Rey Juan Carlos University, c/ Tulipán s/n, 28933, Móstoles, Madrid, Spain*

Abstract

Thermal energy storage systems are a key component of concentrated solar power plants, since its implementation increases the energy generation dispatchability. In particular, thermochemical storage through redox cycles of metal oxides is going to play a major role in future plants working with volumetric air receivers, as they are able to store energy at high temperatures, using air as both heat transfer fluid and reactant. One of the most remarkable characteristics of redox cycles of some metal oxides (e.g. Mn_2O_3/Mn_3O_4 and Co_3O_4/CoO) is that the forward and reverse reactions start at different temperatures, i.e., a thermal hysteresis exists. Namely, the metal oxide reduction takes place at higher temperatures than the re-oxidation of the reduced phase. In the case of Mn-based redox couple, the temperature difference between reduction and oxidation is of ca. 200 ºC, whereas for Co_3O_4/CoO is around 50 ºC. Narrowing the hysteresis loop for the manganese oxide system means that heat is stored and released in a closer range of temperatures, which will suppose an increase of the charge-discharge energy efficiency.
In this work, the effect that co-doping the Mn oxides with Fe and Cu has on the redox temperatures of both reactions has been studied. Materials were prepared by a variation of Pechini method and characterized by XRD and SEM. The capacity to withstand several redox cycles was analyzed by thermogravimetric analyses. It was found that addition of certain amount of both dopants narrowed the thermal hysteresis of such redox couple, presenting stable reversibility.

Peer-review under responsibility of EUROSOLAR - The European Association for Renewable Energy
Keywords: Thermochemical heat storage; manganese oxides; redox cycles; hysteresis; co-doping

* Corresponding author. Tel.: + 917371142
E-mail address: juanmanuel.coronado@imdea.org

Peer-review under responsibility of EUROSOLAR - The European Association for Renewable Energy
doi:10.1016/j.egypro.2015.07.686

1. Introduction

Thermal energy storage systems are attracting high interest for concentrating solar power (CSP) plants since their incorporation allows round-the-clock electricity production, circumventing the problems associated with the inherent intermittence of solar energy. Based on the mechanism in which heat is stored, three different types of systems are identified: sensible, latent and thermochemical heat storage [1,2]. To date, only sensible heat storage has been implemented in commercial CSP plants. However, recent advances in central receiver plants working with volumetric air receivers have focused the attention in the development of thermochemical heat storage (TCS) based on reduction-oxidation cycles of multivalent metal oxides, since with these systems the hot air (>1000 ºC) generated at the receiver can be utilized as both reactant and heat transfer fluid [3–8]. This fact would avoid the need of gas storage as in the case of other TCS approaches based on gas-solid reactions (e.g. decarbonation-carbonation or dehydration-hydration [9]). This type of TCS consists of two main steps. First, part of the hot air generated with sun radiation is used to supply the energy required to perform the thermal reduction of the metal oxide, with its consequent release of oxygen (Equation 1). By this high-temperature endothermic process, energy collected from the sun is partly stored by means of a chemical reaction in the so-called *charge* step. During off-sun periods, *discharge* proceeds by performing the reversible reaction (Equation 2). In this case, air is used to oxidize the reduced form of the metal oxide, releasing the stored heat due to the exothermic nature of this reaction.

Charge $MO_x + \Delta H \rightarrow MO_{x-y} + y/2\ O_2\ (g)$ (1)

Discharge $MO_{x-y} + y/2\ O_2\ (g) \rightarrow MO_x + \Delta H$ (2)

The incorporation of such a type of thermal storage in CSP plants (Fig. 1a) will require the development and evaluation of three major components (Fig. 1b) which are closely interrelated: the storage material, the reactor concept and the system integration.

Regarding the storage material, which is the focus of this work, several factors must be evaluated that in the end could strongly affect to the reactor design and the whole system integration. Among them, energy storage density, cost, toxicity, thermodynamic and kinetics of both reactions and durability of a chosen material are crucial in order to guarantee the feasibility of the TCS system. A preliminary screening of several redox couples was performed by Wong et al.[10]. Based on the aforementioned characteristics they concluded that the most suitable candidates for TCS coupled to CSP plants working with volumetric air receivers were BaO_2/BaO, Co_3O_4/CoO and Mn_2O_3/Mn_3O_4, showing all of them reduction-oxidation reactions in temperatures ranging from 600 to 1000 ºC. In particular, the redox couple Mn_2O_3/Mn_3O_4, which presents the benefit of being an abundant and inexpensive material and with low toxicity, has been proved to withstand several redox cycles at such temperatures [8]. This redox couple stores and releases heat through the next reversible reaction:

$6\ Mn_2O_3 \leftrightarrow 4\ Mn_3O_4 + O_2\ (g) \qquad \Delta H = 202\ kJ/kg$ (3)

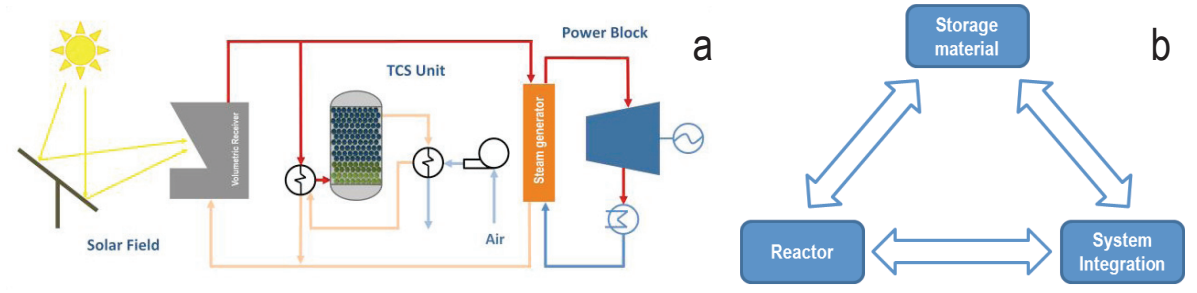

Figure 1. a) Scheme of a thermochemical heat storage system integrated in a CSP plant and b) key components for TCS development

One of the most remarkable characteristics of redox cycles of these metal oxides is that the forward and reverse reactions occur at different temperatures, i.e., a thermal hysteresis exists. Namely, the metal oxide reduction takes place at higher temperatures than the re-oxidation of the reduced phase. In the case of Mn-based redox couple, the temperature difference between reduction and oxidation is of ca. 200 ºC [7], whereas for Co_3O_4/CoO is around 50 ºC range, depending on the nature of the material assayed and the heating ramp used [4–7]. Narrowing the hysteresis loop for the manganese oxide system means that heat is stored and released in a closer range of temperatures, as in the case of Co oxide system, and this fact could suppose an increase of the charge-discharge energy efficiency.

In a previous work [11] we demonstrated that a small addition of Fe shifted the redox reaction to higher temperatures, whereas addition of Cu slightly decreased both values. Therefore, in this work, the influence that co-doping the Mn oxides with Fe and Cu has on the temperatures of both reactions has been studied. Results showed that addition of both metals produced a synergetic effect resulting in a narrowing of the redox hysteresis of the Mn_2O_3/Mn_3O_4 pair.

2. Experimental methods

2.1. Materials preparation

Fe-Cu-doped manganese oxides were prepared by Pechini method, following the procedure described in literature [12]. A certain amount of citric acid (CA) was dissolved into 50 ml of distilled water (Mili-Q) and stirred at 70 ºC until complete dissolution was achieved. Then the metal (Me) precursors were added to the solution with a Me:CA molar ratio of 1:5. The following metal nitrates were used for the synthesis without further purification $Mn(NO_3)_2{\cdot}4\ H_2O$, $Cu(NO_3)_2{\cdot}3\ H_2O$ and $Fe(NO_3)_3{\cdot}9\ H_2O$ (Sigma-Aldrich). After stirring for 3 h at 70 °C, the temperature of the solution was increased to 90 °C, and then ethylene glycol (EG) was added with a molar ratio of CA:EG = 3:2. The resulting solution was further stirred at the same temperature to remove the excess of solvent during 2 h. Then, the obtained resin was subsequently dried in oven at 200 °C for 3 h and then calcined at 450 °C for 4 h in air. Finally, the powders were ground to fine powders with an agate mortar and calcined at 700 ºC for 4 h in static airt.

2.2. Materials characterization

Powder X-ray diffraction (XRD) analyses were carried out employing a Philips PW 3040/00 X'Pert MPD/MRD diffractometer using CuKα radiation (λ = 1.54178 Å) at a scanning rate of 0.2º s^{-1}. The crystallite size was determined from the most intense reflection according to the Scherrer formula.The specific surface area (S_{BET}) was determined by nitrogen adsorption-desorption analyses at 77 K applying the multi-point BET method and using a Quantachrome QuadraSorb-S equipment. Prior to these measurements, samples were degassed at 250 ºC under vacuum. Scanning electron microscopy (SEM) images were taken with a Hitachi TM-100 microscope without any previous treatment of the samples. Stability of redox cycles was monitored by thermogravimetric analysis (TGA) using a SDT Q-600 from TA Instruments. In cyclability studies, ca. 10 mg of sample were placed into 90 µl alumina crucibles and subjected to 30 charging-discharging cycles. Each cycle consisted of a heating step from 650 ºC to 1000 °C and a cooling step from 1000 °C to 650 ºC both at 5 °C min^{-1}, under a constant air flow of 100 ml min^{-1}.

3. Results and discussion

3.1. Structure and morphology of Fe-Cu-doped Mn oxides

A set of six materials was prepared by applying the Pechini method using different Mn:Fe:Cu molar ratios (Table 1). In the case of Cu, amounts higher than 1 % could involve the formation of a segregated phase of Mn-Cu spinel as reported in Mn-Cu-O phase diagram [13]. The presence of a segregated phase is usually undesirable because it is often inert to the redox processes. Accordingly, the mixed oxideacts as a diluting agent, implying that the whole amount of material is not being used for thermochemical storing and, furthermore, it could add kinetic limitations to the redox cycles. Thus, maximum loads of 5 % Cu were used in this study in order to check the aforementioned

hypotheses. In the case of Fe, Ryden et al. [14] showed that increasing the Fe amount shifted the reduction to higher temperature.However, in this case, the better solubility of trivalent iron cations in the bixbyite phase (cubic Mn_2O_3), due to the identical ionic radium of Fe^{3+} and Mn^{3+}in six-fold coordination[15], allowed its incorporation without phase segregation up to a 50 %. Nevertheless, as to avoid increasing the maximum temperature used in the redox cycling runs, the maximum Fe amount used in this work was fixed to 10 % molar.

Table 1: Molar composition, crystal phase, crystallite size (d) and specific surface area (S_{BET}) of each synthesized sample

Sample name	Mn:Fe:Cu (mol %)	Crystal Phase	d (nm)	S_{BET}($m^2 \cdot g^{-1}$)
0Fe-0Cu	100:0:0	Mn_2O_3	50.0	10.4
1Fe-1Cu	98:1:1	Mn_2O_3	41.7	10.0
5Fe-1Cu	94:5:1	Mn_2O_3	37.1	11.8
5Fe-5Cu	90:5:5	Mn_2O_3	43.6	11.2
10Fe-1Cu	89:10:1	Mn_2O_3	43.6	12.2
10Fe-5Cu	85:10:5	Mn_2O_3	44.1	10.9

Figure 2a depicts the XRD diffraction patterns for the six synthesized samples. It can be observed that all of them presented the same reflections, characteristic of bixbyite crystal phase (ICDD-00-041-144). Thus, the formation of any segregated phase due to addition of dopants is not observed, as it could be expected for the samples containing 5 % Cu. Crystallite sizes (Table 2) of the as-synthesized samples were of the same order of magnitude ranging from 37 to 50 nm. Regarding the morphology of the Fe-Cu-doped Mn oxides it was not observed huge differences between the different samples prepared by Pechini method. Figure 2b depicts the SEM micrographs taken to the synthesized materials before being subjected to the charging-discharging cycles. All the samples presented similar shapes, formed by aggregates of irregular particles. Minorchanges were appreciated for the specific surface area. The general trend indicates that addition of Fe slightly enlarged the S_{BET}, whereas increasing amounts of Cu reduced such value (Table 2).

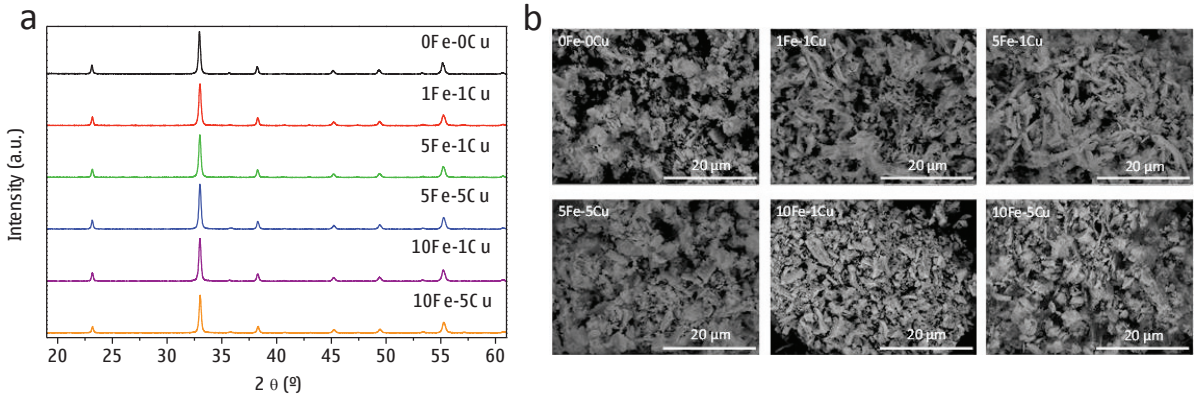

Figure 2.X-Ray diffractograms (a) and SEM micrographs (b) of the as-synthesized Fe-Cu-doped Mn oxides.

3.2. Influence of Fe-Cu doping on the redox thermal hysteresis

As mentioned in the introduction, one of the most remarkable characteristics of redox cycles of transition metal oxides (e.g. Co_3O_4/CoO and Mn_2O_3/Mn_3O_4) is that oxidation and reduction reactions take place at different temperature ranges for the same oxygen partial pressure. For the purpose of narrowing the thermal hysteresis that the Mn_2O_3/Mn_3O_4 pair exhibits, chemical modifications of such materials have been chosen based on previous findings [11], in which we demonstrated that addition of Fe or Cu to the Mn oxides modified the temperatures at which redox reactions take place. In particular, addition of 1 mol % Fe increased both oxidation and reduction temperatures, whereas addition of 1 % Cu had the opposite effect. Thus, in this work we evaluated if the combination of both dopants could have a synergetic effect in such a modification. This effect can be appreciated in Figure 3, where the weight change vs temperature data from TGA runs was plotted for each synthesized sample.

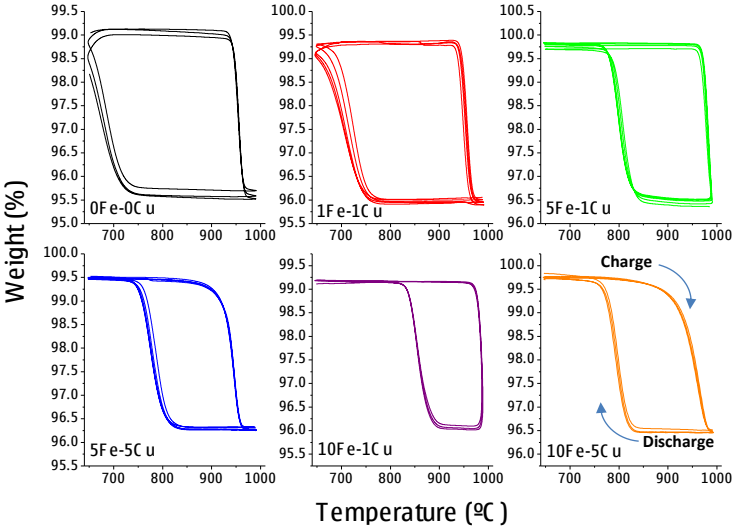

Figure 3.Weight variation versus temperature plot of four redox cycles (2nd to 5th) for the six Fe-Cu-doped Mn oxides. The arrows indicate the cycle direction.

For the un-doped sample (0Fe-0Cu) it can be appreciated that the difference between the onset temperature ofreduction and oxidation (T_{red} and T_{ox} respectively) is 225 ºC (Table 2). By adding 1 mol % of both dopants such difference was reduced by ca. 10 ºC. This was mainly caused by the raise in the T_{ox}, probably due to the incorporation of Fe. Raising the Fe content to 5 % (5Fe-1Cu sample) increased the oxidation temperature to 815 ºC, accompanied by an increase in the reduction temperature, which produced a considerable narrowing in the thermal hysteresis. That effect was even more pronounced when 10 % Fe content was added to the sample (10Fe-1Cu), as the T_{ox} was elevated to 876 ºC and T_{red} to 980 ºC. This fact confirmed the aforementioned trend, since progressive incorporation of Fe into the Mn_2O_3 structure increased both redox temperatures, although Fe-doping specially affected to the oxidation reaction. On the other hand Cu addition decreased both T_{ox} and T_{red}. This can be clearly observed for the two samples with Cu content equal to 5% (5Fe-5Cu and 10Fe-5Cu). In both cases reduction values were lower than for the undoped material. As well its combination with Fe-doping produced a synergetic effect being 10F-5C sample the one that presented the narrowest difference between T_{ox} and T_{red}, namely 98 ºC. It also should be pointed out that addition of Cu change the shape of the weight loss curve, i.e., the kinetics of the reduction of Mn_2O_3. For the samples with just 1 % Cu, it can be appreciated that such weight loss is a fast process, especially during the first part of the reaction. However, for the samples with higher Cu content, the weight loss occurred in a much progressive way, indicating that addition of this dopant slowed the reduction reaction.

Table 2: Reduction and oxidation onset temperaturesand thermal hysteresis value for the fifth redox cycle.

Sample name	T_{red} (ºC)	T_{ox}(ºC)	$\Delta T_{Hysteresis}$(ºC)
0Fe-0Cu	940	715	225
1Fe-1Cu	945	733	212
5Fe-1Cu	972	815	157
5Fe-5Cu	923	803	120
10Fe-1Cu	980	876	104
10Fe-5Cu	914	816	98

3.3. Redox cycles stability

The capacity to withstand several charge-discharge cycles was tested by carrying out 30-redox cycles assays to each sample. The results of these runs are shown in Figure 4. It can be observed that all the Fe-Cu-doped Mn oxides presented redox reversibility in the conditions assayed. However, the two samples with 5 % Cu content, 5Fe-5Cu and 10Fe-5Cu, showed a remarkable change in their cyclability after several charge-discharge steps. For instance, sample 10Fe-5Cu presented a loss in its cycle stability in terms of incomplete reactions. In particular, only an 85 % of the reduced form of such sample was oxidized in the last cycle.

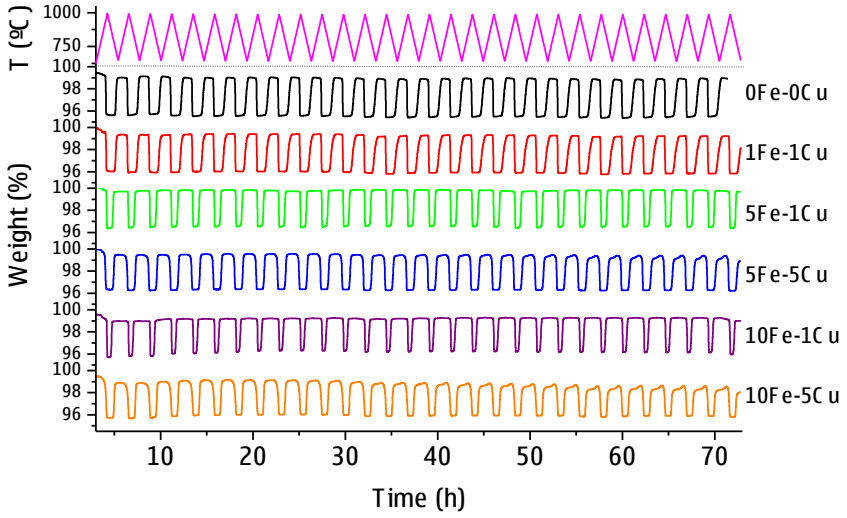

Figure 4. 30 redox cycles analyses performed in thermobalance. Each cycle consisted in heating up to 1000 ºC and cooling down to 650 ºC, under a constant air flow of 100 ml min^{-1}.

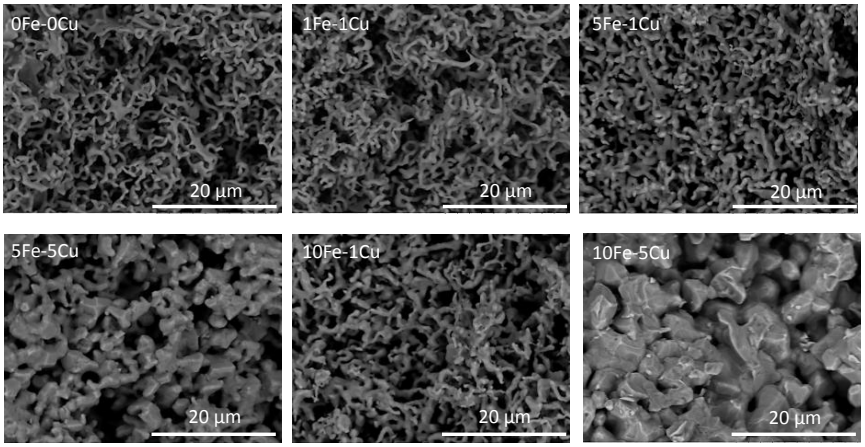

Figure 5.SEM micrographs of the Fe-Cu-doped Mn oxides after 30 redox cycles.

In order to evaluate the morphological changes caused by thermal cycling, SEM pictures were taken to each sample after the 30 redox cycles. As it can be seen in Figure 5, Fe-Cu-doped Mn oxides suffered a remarkable change due to the high temperature at which charge-discharge cycles take place. Namely, materials suffered from particle sintering after cycling; process mainly associated with particle densification and coarsening. The result of these two phenomena is an oxide with open macroporosity and a characteristic coral-like shape. Fe-Cu-doped materials exhibited a similar morphology compared to the un-doped Mn oxide, except for the samples with a 5 % of Cu content. In that case, the sintered particles showed a higher degree of coarsening, being 10Fe-5Cu sample the one with the highest grain size. This remarkable increase in the grain size for that sample, may be the reason why at some point during the cyclability test the oxidation reaction did not achieve full conversion, since this huge morphological change added barriers to the diffusion of oxygen through the reduced form of the metal oxide modifying the overall reaction kinetics. Additionally, for these samples with 5 % Cu, the severe thermal treatment at which they were subjected could cause the formation of a segregated phase of Mn-Cu spinel. The presence of this phase could be also related with the fact that full conversions were not reached, since the whole sample is not participating in the redox reaction. As well, the presence of a segregated phase may favor coarsening and densification phenomena, increasing the particle sintering extent.

3.4. Influence of Fe-Cu-doping on the redox kinetics

As mentioned above, sintering processes, related with particle coarsening and densification, have a direct impact on the oxidation reaction. However, it was found that by doping with the proper amount of Fe and Cu, the diffusional hurdles caused by sintering can be counteracted. This can be observed in Figure 6a, where the cycle-to-cycle evolution of the oxidation rate for each sample is depicted. It can be distinguished three different trends depending on the doping content. That is, 0Fe-0Cu and 1Fe-1Cu samples (low dopant content) presented an exponential decrease of the oxidation rate valuesduring the first part of the cycling run, reaching a plateau on the last half of the assay. For the undoped material, the oxidation rate decrease to the half of its initial value after the 30 redox cycle assay. This exponential decrease can be remarkably improved by the addition of 5 % Fe and 1 % Cu. This sample, not only presented the fastest oxidation rate values over the 30-cycles run, but also, the most stable of all the samples assayed, presenting an oxidation rate average value of 4.3 $\mu molO_2\ min^{-1}\ g^{-1}$. 10Fe-1Cu sample, which showed the fastest oxidation on the first cycle, experienced a gradual decrease during the ten first cycles, period after which presented a stabilization of the oxidation rate values. The two samples with 5 % Cu, 5Fe-5Cu and 10Fe-5Cu, suffered a progressive decrease of the oxidation rate values. This behavior can be related with the oxidation conversions decrease observed for these two samples in the redox cycling tests (Figure 4). Despite such samples presented a higher sintering extent (Figure 5) in comparison with the undoped oxide, they presented faster oxidation reactions, fact that could be explained by the presence of dopants in the Mn_3O_4 lattice.

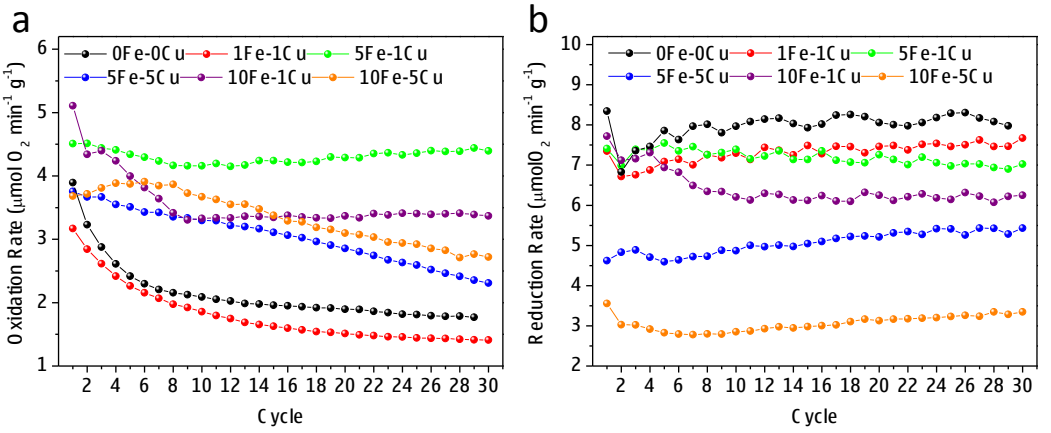

Figure 6.30-cycle oxidation (a) and reduction (b) rate evolution.

Conversely, reduction rates presented fairly stable values over the 30-redox cycle run (Figure 6b). We attributed [8] this fact to the different mechanisms that control oxidation and reduction reactions. In the case of reduction, sintering is not affecting to its rate stability over long thermal cycling in the same extent as for oxidation. In general, reduction is a faster process than oxidation. For instance, for 0Fe-0Cu, in the first cycle reduction is a 2-fold faster reaction than oxidation. However, increasing the Cu content balanced such differences. This was due to slower reduction reactions caused by increasing Cu content. In particular, 10Fe-5Cu sample presented slower reduction reactions over the whole cycling period studied.

In summary, it seems that Fe is the responsible for the oxidation rate enhancement and stabilization over long thermal cycling, whereas increased Cu content caused slower reduction reactions.

4. Conclusions

In this work it was proven that by simultaneously doping the Mn oxides with Cu and Fe it was possible to tune the temperature at which the redox reactions of the system Mn_2O_3/Mn_3O_4 take place, narrowing significantly the characteristic thermal hysteresis of such a redox pair. Moreover, Fe-Cu doped materials, especially those with 1 % Cu, showed stable redox cycles over long-term operation. In particular, incorporation of 5 % Fe and 1 % Cu, produced faster and more stable reaction rates, fact that makes such material a promising candidate for thermal energy storage applications at high temperatures.

Acknowledgements

This work has received financial support from the projects TCS Power of the FP7 (ENERGY.2011.2.5-1) and MULTISTOR (ENE2012-36937) of the Spanish Ministry of Economy and Competiveness.

References

[1]S. Kuravi, J. Trahan, D.Y. Goswami, M.M. Rahman, E.K. Stefanakos, Thermal energy storage technologies and systems for concentrating solar power plants, Prog. Energy Combust. Sci. 39 (2013) 285–319.

[2]A. Gil, M. Medrano, I. Martorell, A. Lázaro, P. Dolado, B. Zalba, et al., State of the art on high temperature thermal energy storage for power generation. Part 1—Concepts, materials and modellization, Renew. Sustain. Energy Rev. 14 (2010) 31–55.

[3]M. Neises, S. Tescari, L. de Oliveira, M. Roeb, C. Sattler, B. Wong, Solar-heated rotary kiln for thermochemical energy storage, Sol. Energy. 86 (2012) 3040–3048.

[4]T. Block, N. Knoblauch, M. Schmücker, The cobalt-oxide/iron-oxide binary system for use as high temperature thermochemical energy storage material, Thermochim. Acta. 577 (2013) 25–32.

[5]C. Agrafiotis, M. Roeb, M. Schmücker, C. Sattler, Exploitation of thermochemical cycles based on solid oxide redox systems for thermochemical storage of solar heat. Part 1: Testing of cobalt oxide-based powders, Sol. Energy. 102 (2014) 189–211.
[6]C. Pagkoura, G. Karagiannakis, A. Zygogianni, S. Lorentzou, M. Kostoglou, A.G. Konstandopoulos, et al., Cobalt oxide based structured bodies as redox thermochemical heat storage medium for future CSP plants, Sol. Energy. 108 (2014) 146–163..
[7]A.J. Carrillo, J. Moya, A. Bayón, P. Jana, V.A. de la Peña O'Shea, M. Romero, et al., Thermochemical energy storage at high temperature via redox cycles of Mn and Co oxides: Pure oxides versus mixed ones, Sol. Energy Mater. Sol. Cells. 123 (2014) 47–57.
[8]A.J. Carrillo, D.P. Serrano, P. Pizarro, J.M. Coronado, Thermochemical heat storage based on the Mn_2O_3/Mn_3O_4 redox couple: influence of the initial particle size on the morphological evolution and cyclability, J. Mater. Chem. A. 2 (2014) 19435–19443.
[9]P. Pardo, A. Deydier, Z. Anxionnaz-Minvielle, S. Rougé, M. Cabassud, P. Cognet, A review on high temperature thermochemical heat energy storage, Renew. Sustain. Energy Rev. 32 (2014) 591–610.
[10]B. Wong, L. Brown, F. Schaube, R. Tamme, C. Sattler, Oxide Based Thermochemical Heat Storage, in: 16th Sol. PACES Int. Symp. Perpignan. Fr., 2010: pp. 1–8.
[11]A.J. Carrillo, D.P. Serrano, P. Pizarro, J.M. Coronado, Improving the performance of thermochemical heat storage at high temperatures based on redox metal oxides, in: Eurotherm Semin. #99 Adv. Therm. Energy Storage, Lleida, Spain, 2014: pp. 1–8.
[12]P. Jana, V.A. de la Peña O'Shea, J.M. Coronado, D.P. Serrano, Cobalt based catalysts prepared by Pechini method for CO_2-free hydrogen production by methane decomposition, Int. J. Hydrogen Energy. 35 (2010) 10285–10294.
[13]P. Wei, M. Bieringer, L.M.D. Cranswick, A. Petric, In situ high-temperature X-ray and neutron diffraction of Cu-Mn oxide phases, J. Mater. Sci. 45 (2010) 1056–1064.
[14]M. Rydén, H. Leion, T. Mattisson, A. Lyngfelt, Combined oxides as oxygen-carrier material for chemical-looping with oxygen uncoupling, Appl. Energy. 113 (2014) 1924–1932.
[15]R.D. Shannon, Revised effective ionic radii and systematic studies of interatomic distances in halides and chalcogenides, Acta Crystallogr. Sect. A. 32 (1976) 751–767.